Wavelet Energy Signature: Comparison and Analysis

Xiaobin Li[1] and Zheng Tian[2]

[1] Department of Applied Mathematics, Northwestern Polytechnical University, Xi'an, 710072, China
lixiaobin2006@gmail.com
[2] Department of Applied Mathematics, Northwestern Polytechnical University, Xi'an, 710072, China

Abstract. Though wavelet transform based methods have recently raised increasing interests in texture analysis due to their good space and frequency localization, many issues related to the choice of the wavelet basis and texture feature remain unresolved. In this paper, we evaluate the performance of seven wavelet energy signatures and eight wavelet basis for texture discrimination. Experimental results on 111 Brodatz textures show that the feature extracted from high and middle frequency channels is more suitable for texture analysis and the choice of wavelet basis has some influence on texture discrimination.

1 Introduction

Texture analysis has played an important role in many areas including robotic vision, industrial monitoring, remote sensing, assisted medical diagnosis and automated target recognition. There are three primary issues in texture analysis, such as texture classification, texture segmentation and synthesis. Extracting textural features is the main step for analyzing texture.

Many features extraction techniques have been invented in the past for texture analysis, such as features based on gray level co-occurrence matrix [1], features based on run length matrix[2] and singular value decomposition spectrum[3], features based on Gaussian Markov random fields (GMRF) [4] and Gibbs random fields[5] and features based on local linear transformations [6] etc. These methods above are usually restricted to the analysis of spatial interactions over relatively small neighborhoods on a single scale. However, psychovisual studies indicate that the human visual system processed images in a multiscale way and an important aspect of texture is scale [7]. So, as a result, more recently methods based on multi-resolusion or multi-channel analysis such as Gabor filters [8], [9] and wavelet transform [10~13] have received a lot of attention. Though the Gabor filter is famous for its simulation with human vision, the output of Gabor filter banks are not mutually orthogonal, which may result in a significant correlation between textures. Moreover, these transformations are usually not reversible, which limits their applicability for texture synthesis. As a preferred tool for multiresolution analysis, wavelet theory provides a more formal, solid and unified approach to multiresolution representation [14], [15].

I. King et al. (Eds.): ICONIP 2006, Part II, LNCS 4233, pp. 474 – 480, 2006.

Many wavelet transform based features have been invented. Among them are wavelet energy signature (WES) which is the most popular feature used in wavelet texture analysis [12]. Despite the empirical success, the choices of wavelet basis (WB) and WES remain unsolved. The impact of the WB has been partially addressed in recently published papers. For example, in [16], Chang and Kuo have suggested that the filter selection has little information on the texture classification. But, on the other hand, the experiments in [17], [18] imply that it is an important issue the choice of filter bank in the wavelet texture characterization. In this paper we analyze the performance of seven WESs, which are combinations of features extracted from different frequency bands, and eight WBs on 111 Brodatz textures [19]. The primary aim is to investigate which frequency bands play an important role in texture description and whether the choice of WB can influence the texture discrimination. This paper is organized as follows. Section 2 presents the basic concept of the wavelet transform. Section 3 gives the methodology and experiment results. Conclusions are given in section 4.

2 Wavelet Transforms

The wavelet transform performs the decomposition of a signal f with a family of function $\psi_{m,n}(x)$ obtained through translation and dilation of a kernel function called mother wavelet via

$$\psi_{m,n}(x) = 2^{-m/2}\psi(2^{-m}x - n). \tag{1}$$

The mother wavelet can be constructed from two-scale difference equations

$$\phi(x) = \sqrt{2}\sum_k h(k)\phi(2x - k), \tag{2}$$

$$\psi(x) = \sqrt{2}\sum_k g(k)\phi(2x - k), \tag{3}$$

where $\phi(x)$ is called scaling function , and $h(k)$ and $g(k)$ can be viewed as filter coefficients of half band low-pass and high-pass filters, respectively.

The filter coefficients $h(k)$ and $g(k)$ play a very crucial role in discrete wavelet transform (DWT) and they can be used for DWT computation instead of the explicit forms for $\phi(x)$ and $\psi(x)$. In fact, a J -level wavelet decomposition can be written as

$$f_0(x) = \sum_k c_{0,k}\varphi_{0,k}(x) \tag{4}$$

$$= \sum_k (c_{J+1,k}\varphi_{J+1,k}(x) + \sum_{j=0}^{J} d_{J+1,k}\psi_{J+1,k}(x)), \tag{5}$$

where coefficients $c_{0,k}$ are given and

$$c_{j+1,n} = \sum_k c_{j,k} h(k - 2n), \tag{6}$$

$$d_{j+1,n} = \sum_k d_{j,k} g(k - 2n). \tag{7}$$

The above two formulas provides a recursive algorithm for wavelet decomposition through filter coefficients $h(k)$ and $g(k)$. The final output of DWT of a signal include a set of detail coefficients $d_{j,k}$ and approximation coefficients $c_{j,k}$.

A two-dimensional DWT can be treated as two one-dimensional transforms over image rows and columns separately. This will generate three orientation selective detail subimages $D_j^{(k)}, k = h, v, d$ and an approximate subimage A_j where j denotes the decomposition level. The process then repeated on the approximate subimage to produce the next level of the resolution. Figure 1 shows a two-level hierarchical decomposition.

Since textures, either micro or macro, have non-uniform gray level variations, they are statistically characterized by the features derived from transformed coefficients in approximation and detail subimages. In other words, we can use these features to analyze the texture.

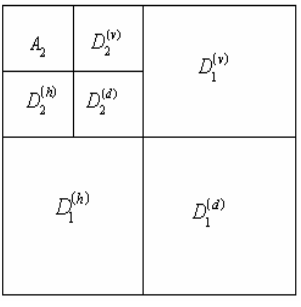

Fig. 1. Wavelet representation of image by detail subimages and approximate subimage

3 Comparison and Analysis

Wavelet texture analysis is considered to be the current state of the art among other texture analysis methods and has shown better performance than other methods in many cases. In this section, we evaluate the performance of seven WESs and eight WBs by using 111 Brodatz textures, each with a size of 75×75 pixels and 256 gray levels. Fig. 2 illustrates some textures from our experimental set. The eight WBs are Haar wavelet, Db2 wavelet, Db4 wavelet, Db7 wavelet, Coif2 wavelet, Bior 2.6 wavelet and Dmey wavelet.

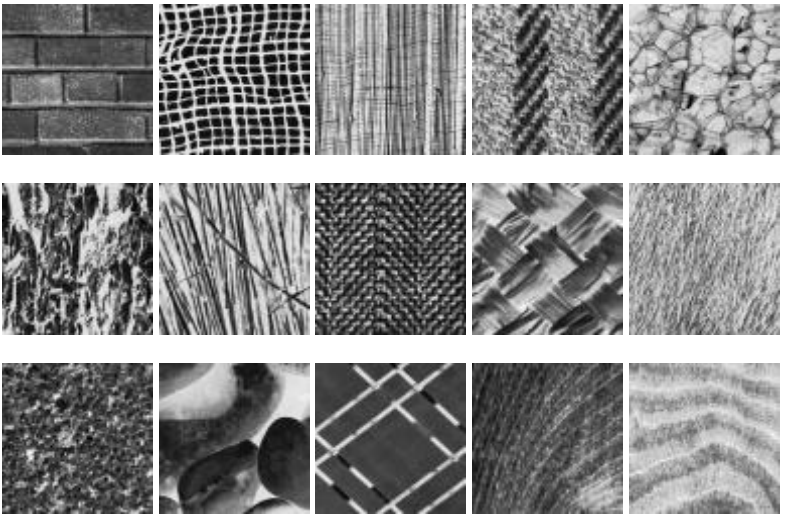

Fig. 2. Some textures from the experimental set

Table 1. Seven wavelet energy signatures

F_1	$\left(\frac{\|A_2\|_F^2}{ared(A_2)}, \frac{\|D_2^{(h)}\|_F^2}{ared(D_2^{(h)})}, \frac{\|D_2^{(v)}\|_F^2}{ared(D_2^{(v)})}, \frac{\|D_2^{(d)}\|_F^2}{ared(D_2^{(d)})}, \frac{\|D_1^{(h)}\|_F^2}{ared(D_1^{(h)})}, \frac{\|D_1^{(v)}\|_F^2}{ared(D_1^{(v)})}, \frac{\|D_1^{(d)}\|_F^2}{ared(D_1^{(d)})} \right)$
F_2	$\left(\frac{\|D_1^{(h)}\|_F^2}{ared(D_1^{(h)})}, \frac{\|D_1^{(v)}\|_F^2}{ared(D_1^{(v)})}, \frac{\|D_1^{(d)}\|_F^2}{ared(D_1^{(d)})} \right)$
F_3	$\left(\frac{\|D_2^{(h)}\|_F^2}{ared(D_2^{(h)})}, \frac{\|D_2^{(v)}\|_F^2}{ared(D_2^{(v)})}, \frac{\|D_2^{(d)}\|_F^2}{ared(D_2^{(d)})}, \frac{\|D_1^{(h)}\|_F^2}{ared(D_1^{(h)})}, \frac{\|D_1^{(v)}\|_F^2}{ared(D_1^{(v)})}, \frac{\|D_1^{(d)}\|_F^2}{ared(D_1^{(d)})} \right)$
F_4	$\left(\frac{\|D_1^{(h)}\|_F^2}{ared(D_1^{(h)})}, \frac{\|D_1^{(v)}\|_F^2}{ared(D_1^{(v)})}, \frac{\|D_1^{(d)}\|_F^2}{ared(D_1^{(d)})}, \frac{\|D_2^{(d)}\|_F^2}{ared(D_2^{(d)})} \right)$
F_5	$\left(\frac{\|A_2\|_F^2}{ared(A_2)}, \frac{\|D_1^{(h)}\|_F^2}{ared(D_1^{(h)})}, \frac{\|D_1^{(v)}\|_F^2}{ared(D_1^{(v)})}, \frac{\|D_1^{(d)}\|_F^2}{ared(D_1^{(d)})} \right)$
F_6	$\left(\frac{\|A_2\|_F^2}{ared(A_2)}, \frac{\|D_2^{(h)}\|_F^2}{ared(D_2^{(h)})}, \frac{\|D_2^{(v)}\|_F^2}{ared(D_2^{(v)})}, \frac{\|D_2^{(d)}\|_F^2}{ared(D_2^{(d)})} \right)$
F_7	$\left(\frac{\|D_2^{(h)}\|_F^2}{ared(D_2^{(h)})}, \frac{\|D_2^{(v)}\|_F^2}{ared(D_2^{(v)})}, \frac{\|D_2^{(d)}\|_F^2}{ared(D_2^{(d)})} \right)$

3.1 Texture Features Selection

The two-level DWT is firstly applied to the texture image. This generates six detail subimages and one approximation subimage. Then the normalized energy of each subimage is calculated and some of them are employed as elements of the texture feature vector. In our test, we choose seven WESs which are given in table I, where $\|\bullet\|_F$ denotes the Frobenius norm and $area(\bullet)$ denotes the product of row number and column number of a matrix.

3.2 Performance Evaluation

For every WB, firstly, we select randomly 20 texture images from 111 Brodatz texture images. Then we extract feature vector $F_i(i = 1, 2, \cdots, 6)$ from each texture image. For F_i, this results in 20 vectors. The cosine of angle of every two of 20 vectors is computed and 190 values are got. Finally, the mean and variance of these 190 values, denoted by $mean(F_i)$ and $\mathrm{var}(F_i)$, are calculated to show the performance of feature F_i. At the same time the best feature for every WB is given. In our experiments, since the variation of seven $\mathrm{var}(F_i)s$ is small, we choose the feature corresponding to the minimal $mean(F_i)$ as the best choice for every WB. To derive some significant statistics, this experiment was repeated 100 times. Table II shows the experimental results, Where $Angle = \arccos(\min_{1\le i\le 6}\{\frac{1}{100}\sum mean(F_i)\})$. In 100 experiments, a surprising thing is for every WB the best feature is same at each time, so Table II also shows the best feature for every wavelet.

From the experiment results, one thing is obvious that for eight WBs the best features are all F_4 which extracted from the detail subimages $D_1^{(j)}(j = h, v, d)$ and $D_2^{(d)}$. This shows that the texture characteristic are mainly in high and middle frequency regions. The other thing is $Angle$ s for eight WBs all lie in the interval $[34^o, 40^o]$, this shows the ability of WB for texture discrimination. If set

$$MaxA = \max\{Angle\}, MinA = \min\{Angle\}, \tag{8}$$

then

$$\frac{MaxA - MinA}{\frac{1}{8}\sum Angle} = 0.1072. \tag{9}$$

This shows that in wavelet texture characterization the choice of WB could affect the texture discrimination. Especially, in eight WBs, Haar wavelet is the most unsuitable for texture discrimination and in contrast Db7 wavelet is the best.

Table 2. The experimental results

WB	Haar	Db2	Db4	Db7
$Angle$ (degree)	35.0888	36.8757	38.4868	39.1391
Feature	F4	F4	F4	F4
WB	Sym8	Coif2	Bior2.6	Dmey
$Angle$ (degree)	38.3809	38.8173	36.6914	38.8966
Feature	F4	F4	F4	F4

4 Conclusions

In this paper we evaluate the performance of seven WESs and eight WBs for texture discrimination. Our experiment results show that in the wavelet texture characterization the choice of WB could influence the texture discrimination. Our findings, that feature F_4 is more suitable for texture analysis than other six features which are used in many other studies, show that the texture characteristic are mainly in high and middle frequency regions. This result can be used for feature selection in the design of system for texture description and synthesis and other areas, such as image coding.

Acknowledgment

This work is supported by the National Natural Science Foundation of China (60375003) , Aeronautics and Astronautics Basal Science Foundation of China (03I53059).

References

1. Haralick, R.M., Shanmugam, K.K., Dinstein, L.: Features for Image Classification. IEEE Trans. Syst. Cyb. 8 (6) (1973) 610–621.
2. Galloway, M. M.: Texture Analysis Using Gray Level Run Lengths," Comput. Graphics Image Process. Vol. 4 (1975) 172–179.
3. Ashjari, B.: Singular Value Decomposition Texture Measurement for Image Classification, PhD, thesis, University of Southern Califomia, Los Angeles, CA, (1982).
4. Cross, G.R., Jain, A.K.: Markov Random Field Texture Models. IEEE Trans. Pattern Anal. Machine Intell. PAMI-5(1) (1983) 25–39.
5. Derin, H., Elliot, H.: Model and Segmentation of Noisy and Textured Images Using Gibbs random Fields. IEEE Trans. Pattern Anal. Machine Intell. PAMI-1 (1987) 251-259.
6. Unser, M.: Local Linear Transforms for Texture Measurements. Signal Process. Vol. 11 (1986) 61–79.

7. Daugman, J.G.: An Information-theoretic View of Analog Representation in Striate Cortex. Comp. Neurosc. (1990) 403-424.
8. Bovik, A. C., Clark, M., and Geisler, W. S.: Multichannel Texture Analysis Using Localized Spatial Filters. IEEE Trans. PAMI, Vol. 12 (1990) 55-73.
9. Jain, A. K. and Farrokhnia, F.: Unsupervised Texture Segmentation Using Gabor Fillters. Pattern Recognition, Vol. 24 (1991) 1167-1186.
10. Arivazhagan, S. and Ganesan, L.: Texture Classification Using Wavelet Transform. Pattern Recogn. Lett. Vol.24 (2003) 1513–1521.
11. Arivazhagan, S. and Ganesan, L.: Texture Segmentation Using Wavelet Transform. Pattern Recogn. Lett. Vol. 24 (2003) 3197–3203.
12. Bharati, M. H., Liu, J. J. and Macgregor, J. F.: Image Texture Analysis: Methods and Comparisons. Chemometrics and intelligent laboratory systems, Vol. 72 (2004) 57-71.
13. Mor, E. and Aladjem, M.: Boundary Refinements for Wavelet-domain Multiscale Texture Segmentation. Image and Vision Computing, Vol. 23 (2005) 1150-1158.
14. Mallat, S.: A Theory for Multiresolution Signal Decomposition: the Wavelet Representation. IEEE Trans. PAMI, Vol.11 (7) (1989) 674-693.
15. Daubechies, I.: Ten Lectures on Wavelets. Philadelphia, PA: SIAM (1992).
16. Chang, T. and Kuo, C.-C. J.: Texture Analysis and Classification with Tree-structured Wavelet Transform. IEEE Trans. Image Processing, Vol. 2(4) (1993) 429-441.
17. Unser, M.: Texture Classification and Segmentation Using Wavelet Frames. IEEE Transactions on Image Processing, Vol.4 (11) (1995) 1549-1560.
18. Mojsilović, A., Popović, M. V. and Rackov, D. M.: On the Selection of an Optimal Wavelet Basis for Texture Characterization. IEEE Transactions on Image Processing, Vol.9 (12) (2000) 2043-2050.
19. Brodatz, P.: Textures, a Photographic Album for Artists and Designers. Dover Publications, New York (1966).